Available online at www.sciencedirect.com
SCIENCE DIRECT®
PERGAMON
International Journal of Mechanical Sciences 45 (2003) 1–20
International Journal of MECHANICAL SCIENCES
www.elsevier.com/locate/ijmecsci

Stress singularities at angular corners in first-order shear deformation plate theory

C.S. Huang*

Department of Civil Engineering, National Chiao Tung University, 1001 Ta-Hsueh Rd., Hsinchu 30050, Taiwan

Received 1 February 2002; received in revised form 19 February 2003; accepted 22 February 2003

Abstract

The first-known Williams-type singularities caused by homogeneous boundary conditions in the first-order shear deformation plate theory (FSDPT) are thoroughly examined. An eigenfunction expansion method is used to solve the three equilibrium equations in terms of displacement components. Asymptotic solutions for both moment singularity and shear-force singularity are developed. The characteristic equations for moment singularity and shear-force singularity and the corresponding corner functions due to ten different combinations of boundary conditions are explicated in this study. The validity of the present solution is confirmed by comparing with the singularities in the exact solution for free vibrations of Mindlin sector plates with simply supported radial edges, and with the singularities in the three-dimensional elasticity solution for a completely free wedge. The singularity orders of moments and shear forces caused by various boundary conditions are also thoroughly discussed. The singularity orders of moments and shear forces are compared according to FSDPT and classic plate theory.

Keywords: Stress singularities; First-order shear deformation plate theory (FSDPT); Eigenfunction expansion

1. Introduction

Stress singularities in elastic plates frequently arise due to boundary conditions along the plate edges and the geometry of the plates. As well known, stress singularities exist at sharp corners in plates with V-notches or with irregular shapes of holes. Analytically determining the stress singularity behavior at a sharp corner is important not only for fracture mechanics [1] but also for numerical analysis of any complex problem involving such a sharp corner [2,3].

* Tel.: +886-3-5712121 ext 54962; fax: +886-3-5716257.
E-mail address: cshuang@cc.nctu.edu.tw (C.S. Huang).

0020-7403/03/$ - see front matter
doi:10.1016/S0020-7403(03)00046-8

Nomenclature

D	flexural rigidity
E	modulus of elasticity
G	shear modulus
h	thickness of plate
$M_r, M_\theta, M_{r\theta}$	moments
Q_r, Q_θ	shear forces
r	radial coordinate
W	transverse displacement of the mid-plane
Ψ_r	bending rotation of the mid-plane in the radial direction
Ψ_θ	bending rotation of the mid-plane in the circumferential direction
α	vertex angle
θ	circular coordinate
υ	Poisson's ratio
κ^2	shear correction factor

Some studies on stress singularities in plates have been undertaken according to classical plate theory or the plane stress assumption. Williams [4,5] pioneered the investigation of stress singularities of homogeneous, isotropic sector plates under bending and in-plane extension, due to various homogeneous boundary conditions. Williams and Chapkis [6] further considered the stress singularities for polarly orthotropic thin plates. Dempsey and Sinclair [7] proposed a new form of Airy stress function to reexamine the stress singularities in isotropic elastic plates under extension. Hein and Erdogan [8] and Bogy and Wang [9] used the Mellin transformation to study the stress singularities for bimaterial wedges, while Dempsey and Sinclair [10] used an Airy stress function for the same purpose. Meanwhile, Ting and Chou [11] applied Stroh's approach [12] to examine the stress singularities at the vertex of anisotropic wedges under extension. Applying classical lamination theory, Ojikutu et al. [13] considered stress singularities at the apex of a laminated composite wedge with simply supported radial edges.

The stress singularities at the corners of moderately thick plates have seldom been addressed. Burton and Sinclair [14] considered the singularities due to six different combinations of homogeneous boundary conditions around a corner, for Reissner's theory. The authors reduced the three field equations of Reissner's theory to two Cauchy–Riemann equations by introducing a stress potential. Williams' procedure was then applied to find equations characterizing the stress singularity behaviors. However, moment singularities but no shear-force singularities were found in their solution. Based on the Mindlin plate theory, Huang et al. [15] investigated the stress singularities at the vertex of a sector plate with simply supported radial edges by finding the exact solution for free vibrations of such a plate. That solution yielded both the moment singularity and the shear-force singularity. The great similarity between Reissner's theory [16] and Mindlin's theory [17] leads one to expect very similar singular behaviors according to these two theories. Consequently, the singularity behaviors in thick plate theories require further study to resolve the conflicts between the conclusions of Burton and Sinclair [14] and those of Huang et al. [15].

This study thoroughly investigates the Williams type stress singularities in first-order shear deformation plate theory (FSDPT) due to ten different combinations of homogeneous boundary conditions. The three field equations in the FSDPT are directly solved by adopting the eigenfunction expansion method recently proposed by Xie and Chaudhuri [18,19] for studying stress singularities in a three-dimensional problem. Notably, the method proposed by Xie and Chaudhuri [18,19] provides the same three-dimensional asymptotic stress fields in the vicinity of the front of crack as those obtained by Hartranft and Sih [20], even though the solution methodology used by Hartranft and Sih [20] is more complex than Xie and Chaudhuri's [18,19]. This study explicates not only the equations characterizing the moment and shear-force singularities, but also the corresponding asymptotic displacement fields for stress singularities. The singularity orders of moments and shear-force variations with the corner angles are graphically depicted for the various homogeneous boundary conditions. The obtained stress singularity orders are compared with those published in different theories or approaches, and especially in Williams' solution [4] for a thin plate.

2. Basic formulation

The equilibrium equations with no external loading, in terms of stress resultants in polar coordinates in the FSDPT are given (cf. [21]),

$$\begin{aligned} &M_{r,r} + \frac{1}{r} M_{r\theta,\theta} + \frac{M_r - M_\theta}{r} - Q_r = 0, \\ &M_{r\theta,r} + \frac{1}{r} M_{\theta,\theta} + \frac{2M_{r\theta}}{r} - Q_\theta = 0, \\ &Q_{r,r} + \frac{Q_r}{r} + \frac{1}{r} Q_{\theta,\theta} = 0, \end{aligned} \tag{1}$$

where the subscript, "j" refers to a partial differential with respect to independent variable j. The stress resultants are related to the transverse displacement and bending rotations by

$$\begin{aligned} M_r &= -D[\Psi_{r,r} + \upsilon r^{-1}(\Psi_r + \Psi_{\theta,\theta})], \\ M_\theta &= -D[r^{-1}(\Psi_r + \Psi_{\theta,\theta}) + \upsilon \Psi_{r,r}], \\ M_{r\theta} &= -\frac{(1-\upsilon)D}{2}[r^{-1}(\Psi_{r,\theta} - \Psi_\theta) + \Psi_{\theta,r}], \\ Q_r &= \kappa^2 Gh(-\Psi_r + W_{,r}), \\ Q_\theta &= \kappa^2 Gh(-\Psi_\theta + r^{-1} W_{,\theta}), \end{aligned} \tag{2}$$

where W is the transverse displacement of the midplane; Ψ_r and Ψ_θ are the bending rotation of the mid-plane normal in the radial and circumferential directions, respectively, h is the thickness of the plate; $D = Eh^3/12(1-\upsilon^2)$ is the flexural rigidity; E is the modulus of elasticity; υ is Poisson's ratio; κ^2 is the shear correction factor, and G is the shear modulus. Reissner [16] took $\frac{5}{6}$ as the value of κ^2, while Mindlin [17] employed $\pi^2/12$.

Substituting Eq. (2) into Eq. (1) yields the equilibrium equation in terms of displacement components:

$$\frac{D}{2}\{(1-\upsilon)(\Psi_{r,rr}+r^{-1}\Psi_{r,r}+r^{-2}\Psi_{r,\theta\theta}-r^{-2}\Psi_r-2r^{-2}\Psi_{\theta,\theta}) +(1+\upsilon)(\Psi_{r,rr}-r^{-2}\Psi_r+r^{-1}\Psi_{r,r}-r^{-2}\Psi_{\theta,\theta}+r^{-1}\Psi_{\theta,\theta r})\} +\kappa^2 Gh(-\Psi_r+W_{,r})=0, \tag{3a}$$

$$\frac{D}{2}\{(1-\upsilon)(\Psi_{\theta,rr}+r^{-1}\Psi_{\theta,r}+r^{-2}\Psi_{\theta,\theta\theta}-r^{-2}\Psi_\theta+2r^{-2}\Psi_{r,\theta}) +(1+\upsilon)(r^{-2}\Psi_{\theta,\theta\theta}+r^{-2}\Psi_{r,\theta}+r^{-1}\Psi_{r,\theta r})\} +\kappa^2 Gh(-\Psi_\theta+r^{-1}W_{,\theta})=0, \tag{3b}$$

$$\kappa^2 Gh(W_{,rr}+r^{-1}W_{,r}+r^{-2}W_{,\theta\theta}-\Psi_{r,r}-r^{-1}\Psi_r-r^{-1}\Psi_{\theta,\theta})=0. \tag{3c}$$

On the basis of separation of variables, the displacement components are assumed to take the following form:

$$\Psi_r(r,\theta)=\mathrm{e}^{p\theta}\psi_r(r),\quad \Psi_\theta(r,\theta)=\mathrm{e}^{p\theta}\psi_\theta(r)\quad\text{and}\quad W(r,\theta)=\mathrm{e}^{p\theta}w(r), \tag{4}$$

where p is commonly a complex number. Substituting Eq. (4) into Eqs. (3) with careful arrangement yields

$$\frac{D}{2}\{(1-\upsilon)(\psi_r''+r^{-1}\psi_r'-(1+p^2)r^{-2}\psi_r+2pr^{-2}\psi_\theta) +(1+\upsilon)(\psi_r''-r^{-2}\psi_r+r^{-1}\psi_r'-pr^{-2}\psi_\theta+pr^{-1}\psi_\theta')\}+\kappa^2 Gh(-\psi_r+w')=0, \tag{5a}$$

$$\frac{D}{2}\{(1-\upsilon)(\psi_\theta''+r^{-1}\psi_\theta'+(p^2-1)r^{-2}\psi_\theta+2pr^{-2}\psi_r) +(1+\upsilon)(p^2r^{-2}\psi_\theta+pr^{-2}\psi_r+pr^{-1}\psi_r')\}+\kappa^2 Gh(-\psi_\theta+pr^{-1}w)=0, \tag{5b}$$

$$\kappa^2 Gh(w''+r^{-1}w'+p^2r^{-2}w-\psi_r'-r^{-1}\psi_r-pr^{-1}\psi_\theta)=0, \tag{5c}$$

where the primes denote differentials with respect to r. The coupled ordinary differential equations (Eqs. (5)) are solved using the Frobenius method.

3. Singularity of bending moments

Let

$$\psi_r(r)=\sum_{m=0}a_{2m}r^{\lambda+2m},\quad \psi_{\theta(r)}=\sum_{m=0}b_{2m}r^{\lambda+2m}\quad\text{and}\quad w(r)=\sum_{m=0}c_{2m}r^{\lambda+2m+1}, \tag{6}$$

where λ can be a complex number. Obviously, the real part of λ must be larger than zero to satisfy the regularity condition for the displacement components, as r approaches zero. Consequently, the

series given in Eq. (6) can lead to singular moments in the vicinity of r equal to zero, but no singularity for shear forces. Substituting Eq. (6) into Eqs. (5) gives

$$\frac{D}{2}\left\{\sum_{m=0}[(-2+2(2m+\lambda)^2+p^2(1-\upsilon))a_{2m}+p((\lambda+2m)(1+\upsilon)-3+\upsilon)b_{2m}]r^{\lambda+2m-2}\right\}$$
$$+\sum_{m=0}\kappa^2 Gh[-a_{2m}+(\lambda+2m+1)c_{2m}]r^{\lambda+2m}=0, \tag{7a}$$

$$\frac{D}{2}\left\{\sum_{m=0}[(3-\upsilon+(1+\upsilon)(\lambda+2m))pa_{2m}+((1-\upsilon)((\lambda+2m)^2+p^2-1)+(1+\upsilon)p^2)b_{2m}]r^{\lambda+2m-2}\right\}$$
$$+\sum_{m=0}\kappa^2 Gh[-b_{2m}+pc_{2m}]r^{\lambda+2m}=0, \tag{7b}$$

$$\sum_{m=0}[((\lambda+2m+1)^2+p^2)c_{2m}-(\lambda+2m+1)a_{2m}-pb_{2m}]r^{\lambda+2m-1}=0. \tag{7c}$$

Satisfying Eqs. (7) results in coefficients of r with different orders equal to zero. Consequently, a set of recurrent relationships among the coefficients can be attained from the following equations:

$$\frac{D}{2}\{[-2+2(2m+2+\lambda)^2+p^2(1-\upsilon)]a_{2m+2}+p[(\lambda+2m+2)(1+\upsilon)-3+\upsilon]b_{2m+2}\}$$
$$=-\kappa^2 Gh[-a_{2m}+(\lambda+2m+1)c_{2m}], \tag{8a}$$

$$\frac{D}{2}\{[3-\upsilon+(1+\upsilon)(\lambda+2m+2)]pa_{2m+2}+[(1-\upsilon)((\lambda+2m+2)^2+p^2-1)+(1+\upsilon)p^2]b_{2m+2}\}$$
$$=-\kappa^2 Gh[-b_{2m}+pc_{2m}], \tag{8b}$$

$$-(\lambda+2m+3)a_{2m+2}-pb_{2m+2}+[(\lambda+2m+3)^2+p^2]c_{2m+2}=0. \tag{8c}$$

The following three equations can also be established from the coefficients of the lowest order of r in Eqs. (7):

$$[(1-\upsilon)p^2+2\lambda^2-2]a_0+p[(1+\upsilon)\lambda-3+\upsilon)]b_0=0, \tag{9a}$$

$$p[3-\upsilon+(1+\upsilon)\lambda]a_0+[(1-\upsilon)(\lambda^2+p^2-1)+(1+\upsilon)p^2]b_0=0, \tag{9b}$$

$$-(\lambda+1)a_0-pb_0+[(\lambda+1)^2+p^2]c_0=0. \tag{9c}$$

Eqs. (9) are a set of linear homogeneous algebraic equations for a_0, b_0, and c_0. Nontrivial solution results in four distinct roots for p, and they are

$$p=\pm i(\lambda-1) \quad \text{and} \quad p=\pm i(\lambda+1). \tag{10}$$

When $p=\pm i(\lambda+1)$, $b_0=\pm ia_0$, and c_0 is undetermined. When $p=\pm i(\lambda-1)$,

$$b_0=\pm k_1 a_0 \quad \text{and} \quad c_0=\gamma_1 a_0, \tag{11}$$

where

$$k_1 = -\frac{\mathrm{i}[2(1-\upsilon)+(1+\upsilon)(\lambda+1)]}{[2(1-\upsilon)-(1+\upsilon)(\lambda-1)]}, \tag{12a}$$

$$\gamma_1 = \frac{\upsilon-1}{-3+\lambda+\upsilon+\upsilon\lambda}. \tag{12b}$$

Consequently, we can express the solution of Eqs. (3) in the following form:

$$\Psi_r = \mathrm{e}^{\mathrm{i}(\lambda+1)\theta}\sum_{m=0} a_{2m,1} r^{\lambda+2m} + \mathrm{e}^{-\mathrm{i}(\lambda+1)\theta}\sum_{m=0} a_{2m,2} r^{\lambda+2m} + \mathrm{e}^{\mathrm{i}(\lambda-1)\theta}\sum_{m=0} a_{2m,3} r^{\lambda+2m} + \mathrm{e}^{-\mathrm{i}(\lambda-1)\theta}\sum_{m=0} a_{2m,4} r^{\lambda+2m}, \tag{13a}$$

$$\Psi_\theta = \mathrm{e}^{\mathrm{i}(\lambda+1)\theta}\sum_{m=0} b_{2m,1} r^{\lambda+2m} + \mathrm{e}^{-\mathrm{i}(\lambda+1)\theta}\sum_{m=0} b_{2m,2} r^{\lambda+2m} + \mathrm{e}^{\mathrm{i}(\lambda-1)\theta}\sum_{m=0} b_{2m,3} r^{\lambda+2m} + \mathrm{e}^{-\mathrm{i}(\lambda-1)\theta}\sum_{m=0} b_{2m,4} r^{\lambda+2m}, \tag{13b}$$

$$W = \mathrm{e}^{\mathrm{i}(\lambda+1)\theta}\sum_{m=0} c_{2m,1} r^{\lambda+2m+1} + \mathrm{e}^{-\mathrm{i}(\lambda+1)\theta}\sum_{m=0} c_{2m,2} r^{\lambda+2m+1} + \mathrm{e}^{\mathrm{i}(\lambda-1)\theta}\sum_{m=0} c_{2m,3} r^{\lambda+2m+1} + \mathrm{e}^{-\mathrm{i}(\lambda-1)\theta}\sum_{m=0} c_{2m,4} r^{\lambda+2m+1} \tag{13c}$$

where $b_{0,1} = \mathrm{i}a_{0,1}$, $b_{0,2} = -\mathrm{i}a_{0,2}$, $b_{0,3} = k_1 a_{0,3}$, $b_{0,4} = -k_1 a_{0,4}$, $c_{0,3} = \gamma_1 a_{0,3}$, $c_{0,4} = \gamma_1 a_{0,4}$; and $a_{0,1}$, $a_{0,2}$, $a_{0,3}$, $a_{0,4}$, $c_{0,1}$, and $c_{0,2}$ are undetermined. The other coefficients in Eqs. (13) can be determined from Eqs. (8).

To determine the singularity at a corner of a plate, one needs the asymptotic form for the stress resultants. The general asymptotic form for the displacement components can be simply written from Eqs. (13) as follows:

$$\Psi_r(r,\theta) = (A_1\cos(\lambda+1)\theta + A_2\sin(\lambda+1)\theta + A_3\cos(\lambda-1)\theta + A_4\sin(\lambda-1)\theta)r^\lambda + O(r^{\lambda+2}),$$

$$\Psi_\theta(r,\theta) = (A_2\cos(\lambda+1)\theta - A_1\sin(\lambda+1)\theta + k_2A_4\cos(\lambda-1)\theta - k_2A_3\sin(\lambda-1)\theta)r^\lambda + O(r^{\lambda+2}),$$

$$W(r,\theta) = (C_1\cos(\lambda+1)\theta + C_2\sin(\lambda+1)\theta + \gamma_1A_3\cos(\lambda-1)\theta + \gamma_1A_4\sin(\lambda-1)\theta)r^{\lambda+1} + O(r^{\lambda+3}), \tag{14}$$

where $A_1 = a_{0,1} + a_{0,2}, A_2 = \mathrm{i}(a_{0,1} - a_{0,2})$, $A_3 = a_{0,3} + a_{0,4}$, $A_4 = \mathrm{i}(a_{0,3} - a_{0,4})$, $C_1 = c_{0,1} + c_{0,2}$, $C_2 = \mathrm{i}(c_{0,1} - c_{0,2})$, and $k_2 = -\mathrm{i}k_1$. These coefficients are specified by the boundary conditions.

As well known, the stress singularities at the vertex of a sector plate are determined by the radial boundary conditions along the vertex only. In FSDPT, four types of boundary conditions along a radial edge, say $\theta = \theta_0$, can be present:

$$\text{clamped} \quad W(r,\theta_0) = \Psi_r(r,\theta_0) = \Psi_\theta(r,\theta_0) = 0, \tag{15a}$$

$$\text{free} \quad M_\theta(r,\theta_0) = M_{r\theta}(r,\theta_0) = Q_\theta(r,\theta_0) = 0, \tag{15b}$$

$$\text{type I simply supported} \quad W(r,\theta_0) = \Psi_r(r,\theta_0) = M_\theta(r,\theta_0) = 0, \tag{15c}$$

$$\text{type II simply supported} \quad W(r,\theta_0) = M_\theta(r,\theta_0) = M_{r\theta}(r,\theta_0) = 0. \tag{15d}$$

We will describe the procedure for obtaining the characteristic equation for λ, and the corresponding displacement fields in the vicinity of the vertex for the simply supported radial edges, for the sake of demonstration.

Consider a sector plate with vertex angle equal to α. Taking advantage of the symmetry of the problem, substitution of Eq. (14) into Eq. (15c) yields the following equations for symmetric deformation:

$$C_1 \cos(\lambda+1)\alpha/2 + \gamma_1 A_3 \cos(\lambda-1)\alpha/2 = 0, \tag{16a}$$

$$A_1 \cos(\lambda+1)\alpha/2 + A_3 \cos(\lambda-1)\alpha/2 = 0, \tag{16b}$$

$$A_1\lambda(1-\upsilon)\cos(\lambda+1)\alpha/2 + A_3(k_2(\lambda-1) - \lambda\upsilon - 1)\cos(\lambda-1)\alpha/2 = 0. \tag{16c}$$

Ensuring nontrivial solution results in the characteristic equation for λ,

$$(\cos(\lambda-1)\alpha/2)(\cos(\lambda+1)\alpha/2)^2 = 0, \tag{17a}$$

which, without loss of any roots, can be simply written as

$$(\cos(\lambda-1)\alpha/2)(\cos(\lambda+1)\alpha/2) = 0. \tag{17b}$$

When $\cos(\lambda-1)\alpha/2 = 0$, the coefficients A_1 and C_1 are found equal to zero. Accordingly, the resultant asymptotic displacement fields in the vicinity of the vertex of the sector plate ($r \to 0$) are given by

$$\Psi_r(r,\theta) = A_3\gamma^\lambda \cos(\lambda-1)\theta, \quad \Psi_\theta(r,\theta) = -k_2 r^\lambda A_3 \sin(\lambda-1)\theta,$$
$$W(r,\theta) = \gamma_1 A_3 r^{\lambda+1}\cos(\lambda-1)\theta. \tag{18}$$

Similarly, $\cos(\lambda+1)\alpha/2=0$ results in A_3 equal to zero. The corresponding asymptotic displacement fields are

$$\Psi_r(r,\theta) = A_1\gamma^\lambda \cos(\lambda+1)\theta, \quad \Psi_\theta(r,\theta) = -r^\lambda A_1 \sin(\lambda+1)\theta,$$
$$W(r,\theta) = C_1 r^{\lambda+1}\cos(\lambda+1)\theta. \tag{19}$$

These asymptotic displacement fields will be called as "corner functions" below.

By following a procedure similar to that described above, the characteristic equation of λ for anti-symmetric deformation for type I simply-supported radial edges can be determined. The corresponding corner functions are thus obtained. Tables 1 and 2, respectively, summarize the characteristic equations of λ for different combinations of boundary conditions along the radial edges and the corresponding corner functions. In Table 2, the corner functions associated with identical boundary conditions along two radial edges were determined by considering the range, $-\alpha/2 \leqslant \theta \leqslant \alpha/2$ and taking advantage of the problems' symmetry. The other corner functions were determined by considering $0 \leqslant \theta \leqslant \alpha$.

Table 1
Comparison of characteristic equations for FSDPT and classical plate theory (CPT)

Case No.	Boundary conditions	Characteristic equations	
		FSDPT	CPT
1	Simply supported (I)–simply supported (I)	$(\cos(\lambda-1)\alpha/2)(\cos(\lambda+1)\alpha/2)=0\ (S^*)$ $(\sin(\lambda-1)\alpha/2)(\sin(\lambda+1)\alpha/2)=0\ (A^*)$	$\cos\alpha\lambda=-\cos\alpha\ (S^*)$ $\cos\alpha\lambda=+\cos\alpha\ (A^*)$
2	Clamped-free	$\sin^2\lambda\alpha=\frac{4-\lambda^2(1+\upsilon)^2\sin^2\alpha}{(3-\upsilon)(1+\upsilon)}$	$\sin^2\lambda\alpha=\frac{4-\lambda^2(1-\upsilon)^2\sin^2\alpha}{(3+\upsilon)(1-\upsilon)}$
3	Simply supported (I)–free	$\sin 2\lambda\alpha=\lambda\sin 2\alpha$	$\sin 2\lambda\alpha=\frac{\lambda(1-\upsilon)}{-3-\upsilon}\sin 2\alpha$
4	Simply supported (I)–clamped	$\sin 2\lambda\alpha=\frac{\lambda(1+\upsilon)}{-3+\upsilon}\sin 2\alpha$	$\sin 2\lambda\alpha=\lambda\sin 2\alpha$
5	Free–free	$\sin\lambda\alpha=-\lambda\sin\alpha\ (S^*)$ $\sin\lambda\alpha=\lambda\sin\alpha\ (A^*)$	$\sin\lambda\alpha=-\frac{\lambda(1-\upsilon)}{-3-\upsilon}\sin\alpha\ (S^*)$ $\sin\lambda\alpha=\frac{\lambda(1-\upsilon)}{-3-\upsilon}\sin\alpha\ (A^*)$
6	Clamped–Clamped	$\sin\lambda\alpha=-\frac{\lambda(1+\upsilon)}{-3+\upsilon}\sin\alpha\ (S^*)$ $\sin\lambda\alpha=\frac{\lambda(1+\upsilon)}{-3+\upsilon}\sin\alpha\ (A^*)$	$\sin\lambda\alpha=-\lambda\sin\alpha\ (S^*)$ $\sin\lambda\alpha=\lambda\sin\alpha\ (A^*)$
7	Simply supported (II)–simply supported (II)	$\sin\lambda\alpha=-\lambda\sin\alpha\ (S^*)$ $\sin\lambda\alpha=\lambda\sin\alpha\ (A^*)$	
8	Clamped–simply supported (II)	$\sin^2\lambda\alpha=\frac{4-\lambda^2(1+\upsilon)^2}{(3-\upsilon)(1+\upsilon)}\sin^2\alpha$	
9	Simply supported (I)–simply supported (II)	$\sin 2\lambda\alpha=\lambda\sin 2\alpha$	
10	Simply supported (II)–free	$\sin\lambda\alpha=\pm\lambda\sin\alpha$	

Note: $^*S$—symmetric case, A—anti-symmetric case.

Interestingly, Table 1 reveals that the characteristic equations resulting from the free radial edge are the same as those relevant to the type II simply supported boundary conditions. This finding indicates that these characteristic equations are independent of the boundary conditions for W and Q_θ. However, these two types of boundary conditions produced different corner functions for w (see Table 2).

For simplicity, C and F are used to denote the clamped and free boundary conditions, respectively, while S(I) and S(II) denote types I and II simply supported boundary conditions.

As stated before, the real part of λ (Re(λ)) must exceed zero to satisfy the regularity condition for the displacement components, as r approaches zero. Under this restriction, the minimum values of Re(λ) versus the vertex angle (α) for various boundary conditions are shown in Fig. 1. Numerical results were obtained for a Poisson's ratio of 0.3. The relationships between the moments and bending rotations show that the stress singularities occur at the vertex when Re(λ) is below one. The cusps

Table 2
Corner functions corresponding to various boundary conditions

Case no.	Boundary conditions	Corner functions
1	Simply supported (I)–simply supported (I)	(1) $\Psi_r(r,\theta)=A_3\gamma^{\lambda}\cos(\lambda-1)\theta, \Psi_\theta(r,\theta)=-k_2A_3r^{\lambda}\sin(\lambda-1)\theta$ $W(r,\theta)=\gamma_1A_3r^{\lambda+1}\cos(\lambda-1)\theta$ (for $\cos(\lambda-1)\alpha/2=0$) (2) $\Psi_r(r,\theta)=A_1\gamma^{\lambda}\cos(\lambda+1)\theta, \Psi_\theta(r,\theta)=-A_1r^{\lambda}\sin(\lambda+1)\theta$ $W(r,\theta)=C_1r^{\lambda+1}\cos(\lambda+1)\theta$ (for $\cos(\lambda+1)\alpha/2=0$) (3) $\Psi_r(r,\theta)=A_4\gamma^{\lambda}\sin(\lambda-1)\theta, \Psi_\theta(r,\theta)=k_2A_4r^{\lambda}\cos(\lambda-1)\theta$ $W(r,\theta)=\gamma_1A_4r^{\lambda+1}\sin(\lambda-1)\theta$ (for $\sin(\lambda-1)\alpha/2=0$) (4) $\Psi_r(r,\theta)=A_2\gamma^{\lambda}\sin(\lambda+1)\theta, \Psi_\theta(r,\theta)=A_2r^{\lambda}\cos(\lambda+1)\theta$ $W(r,\theta)=C_2r^{\lambda+1}\sin(\lambda+1)\theta$ (for $\sin(\lambda+1)\alpha/2=0$)
2	Clamped–free	$\Psi_r(r,\theta) = A_1r^{\lambda}\{\cos(\lambda+1)\theta-k_2\eta_1\sin(\lambda+1)\theta-\cos(\lambda-1)\theta+\eta_1\sin(\lambda-1)\theta\}$ $\Psi_\theta(r,\theta) = A_1r^{\lambda}\{-\sin(\lambda+1)\theta-k_2\eta_1\cos(\lambda+1)\theta+k_2\sin(\lambda-1)\theta+k_2\eta_1\cos(\lambda-1)\theta\}$ $W(r,\theta) = A_1r^{\lambda+1}\{\gamma_1\cos(\lambda+1)\theta+\eta_2\sin(\lambda+1)\theta-\gamma_1\cos(\lambda-1)\theta+\gamma_1\eta_1\sin(\lambda-1)\theta\}$ $\eta_1=-\frac{\lambda(1-\upsilon)\cos(\lambda+1)\alpha-(k_2(\lambda-1)-\lambda\upsilon-1)\cos(\lambda-1)\alpha}{(k_2(\lambda-1)-\lambda\upsilon-1)\sin(\lambda-1)\alpha-k_2\lambda(1-\upsilon)\sin(\lambda+1)\alpha}$ $\eta_2=\frac{((\lambda+1)\gamma_1-1)\sin(\lambda+1)\alpha-(\lambda\gamma_1-k_2-\gamma_1)(\sin(\lambda-1)\alpha+\eta_1\cos(\lambda-1)\alpha)}{(1+\lambda)\cos(\lambda+1)\alpha}-\frac{k_2\eta_1}{1+\lambda}$
3	Simply supported (I)–free	$\Psi_r(r,\theta)=A_4r^{\lambda}\{\eta_3\sin(\lambda+1)\theta+\sin(\lambda-1)\theta\}$ $\Psi_\theta(r,\theta)=A_4r^{\lambda}\{\eta_3\cos(\lambda+1)\theta+k_2\cos(\lambda-1)\theta\}$ $W(r,\theta)=A_4r^{\lambda+1}\{\eta_4\sin(\lambda+1)\theta+\gamma_1\sin(\lambda-1)\theta\}$ $\eta_3=-\frac{(1+\lambda)(1+\upsilon)}{-3+\lambda+\upsilon+\lambda\upsilon}\frac{\sin(\lambda-1)\alpha}{\sin(\lambda+1)\alpha}$ $\eta_4=\frac{\eta_3\cos(\lambda+1)\alpha+(\lambda\gamma_1-k_2-\gamma_1)\cos(\lambda-1)\alpha}{(\lambda+1)\cos(\lambda+1)\alpha}$
4	Simply supported (I)–clamped	$\Psi_r(r,\theta)=A_4r^{\lambda}\left\{-\frac{\sin(\lambda-1)\alpha}{\sin(\lambda+1)\alpha}\sin(\lambda+1)\theta+\sin(\lambda-1)\theta\right\}$ $\Psi_\theta(r,\theta)=A_4r^{\lambda}\left\{-\frac{\sin(\lambda-1)\alpha}{\sin(\lambda+1)\alpha}\cos(\lambda+1)\theta+k_2\cos(\lambda-1)\theta\right\}$ $W(r,\theta)=A_4\gamma_1r^{\lambda+1}\left\{-\frac{\sin(\lambda-1)\alpha}{\sin(\lambda+1)\alpha}\sin(\lambda+1)\theta+\sin(\lambda-1)\theta\right\}$
5	Free–free	(1) Symmetric case $\Psi_r(r,\theta)=A_3r^{\lambda}\{\eta_5\cos(\lambda+1)\theta+\cos(\lambda-1)\theta\}$ $\Psi_\theta(r,\theta)=A_3r^{\lambda}\{-\eta_5\sin(\lambda+1)\theta-k_2\sin(\lambda-1)\theta\}$ $W(r,\theta)=A_3r^{\lambda+1}\{\eta_6\cos(\lambda+1)\theta+\gamma_1\cos(\lambda-1)\theta\}$ $\eta_5=-\frac{k_2(\lambda-1)-\lambda\upsilon-1}{\lambda(1-\upsilon)}\frac{\cos(\lambda-1)\alpha/2}{\cos(\lambda+1)\alpha/2}$ $\eta_6=\frac{\eta_5}{1+\lambda}-\frac{(\lambda\gamma_1-k_2-\gamma_1)\sin(\lambda-1)\alpha/2}{(1+\lambda)\sin(\lambda+1)\alpha/2}$

Table 2 (*continued*)

Case no.	Boundary conditions	Corner functions
		(2) Anti-symmetric case
		$\Psi_r(r,\theta) = A_4 r^{\lambda}\{\eta_7 \sin(\lambda+1)\theta + \sin(\lambda-1)\theta\}$
		$\Psi_\theta(r,\theta) = A_4 r^{\lambda}\{\eta_7 \cos(\lambda+1)\theta + k_2 \cos(\lambda-1)\theta\}$
		$W(r,\theta) = A_4 r^{\lambda+1}\{\eta_8 \sin(\lambda+1)\theta + \gamma_1 \sin(\lambda-1)\theta\}$
		$\eta_7 = -\frac{k_2(\lambda-1)-\lambda\upsilon-1}{\lambda(1-\upsilon)}\ \frac{\sin(\lambda-1)\alpha/2}{\sin(\lambda+1)\alpha/2}$
		$\eta_8 = \frac{\eta_7}{1+\lambda} - \frac{(\lambda\gamma_1-k_2-\gamma_1)\cos(\lambda-1)\alpha/2}{(1+\lambda)\cos(\lambda+1)\alpha/2}$
6	Clamped-Clamped	(1) Symmetric case
		$\Psi_r(r,\theta) = A_1 r^{\lambda}\{\cos(\lambda+1)\theta - (\cos(\lambda+1)\alpha/2/\cos(\lambda-1)\alpha/2)\cos(\lambda-1)\theta\}$
		$\Psi_\theta(r,\theta) = A_1 r^{\lambda}\{-\sin(\lambda+1)\theta + k_2(\cos(\lambda+1)\alpha/2/\cos(\lambda-1)\alpha/2)\sin(\lambda-1)\theta\}$
		$W(r,\theta) = A_1\gamma_1 r^{\lambda+1}\{\cos(\lambda+1)\theta - (\cos(\lambda+1)\alpha/2/\cos(\lambda-1)\alpha/2)\cos(\lambda-1)\theta\}$
		(2) Anti-symmetric case
		$\Psi_r(r,\theta) = A_2 r^{\lambda}\{\sin(\lambda+1)\theta - (\sin(\lambda+1)\alpha/2/\sin(\lambda-1)\alpha/2)\sin(\lambda-1)\theta\}$
		$\Psi_\theta(r,\theta) = A_2 r^{\lambda}\{\cos(\lambda+1)\theta - k_2(\sin(\lambda+1)\alpha/2/\sin(\lambda-1)\alpha/2)\cos(\lambda-1)\theta\}$
		$W(r,\theta) = A_2\gamma_1 r^{\lambda+1}\{\sin(\lambda+1)\theta - (\sin(\lambda+1)\alpha/2/\sin(\lambda-1)\alpha/2)\sin(\lambda-1)\theta\}$
7	Simply supported (II)–simply supported (II)	(1) symmetric case
		$\Psi_r(r,\theta) = A_3 r^{\lambda}\{\eta_9 \cos(\lambda+1)\theta + \cos(\lambda-1)\theta\}$
		$\Psi_\theta(r,\theta) = A_3 r^{\lambda}\{-\eta_9 \sin(\lambda+1)\theta - k_2 \sin(\lambda-1)\theta\}$
		$W(r,\theta) = A_3\gamma_1 r^{\lambda+1}\{\eta_{10} \cos(\lambda+1)\theta + \cos(\lambda-1)\theta\}$
		$\eta_9 = -\frac{(1+k_2)(\lambda-1)\sin(\lambda-1)\alpha/2}{2\lambda\sin(\lambda+1)\alpha/2}, \quad \eta_{10} = -\frac{\cos(\lambda-1)\alpha/2}{\cos(\lambda+1)\alpha/2}$
		(2) anti-symmetric case
		$\Psi_r(r,\theta) = A_4 r^{\lambda}\{\eta_{11} \sin(\lambda+1)\theta + \sin(\lambda-1)\theta\}$
		$\Psi_\theta(r,\theta) = A_4 r^{\lambda}\{\eta_{11} \cos(\lambda+1)\theta + k_2 \cos(\lambda-1)\theta\}$
		$W(r,\theta) = A_4\gamma_1 r^{\lambda+1}\{\eta_{12} \sin(\lambda+1)\theta + \sin(\lambda-1)\theta\}$
		$\eta_{11} = -\frac{(1+k_2)(\lambda-1)\cos(\lambda-1)\alpha/2}{2\lambda\cos(\lambda+1)\alpha/2}, \quad \eta_{12} = -\frac{\sin(\lambda-1)\alpha/2}{\sin(\lambda+1)\alpha/2}$
8	Clamped–simply supported (II)	$\Psi_r(r,\theta) = A_1 r^{\lambda}\{\cos(\lambda+1)\theta - k_2\eta_1 \sin(\lambda+1)\theta - \cos(\lambda-1)\theta + \eta_1 \sin(\lambda-1)\theta\}$
		$\Psi_\theta(r,\theta) = A_1 r^{\lambda}\{-\sin(\lambda+1)\theta - k_2\eta_1 \cos(\lambda+1)\theta + k_2 \sin(\lambda-1)\theta + k_2\eta_1 \cos(\lambda-1)\theta\}$
		$W(r,\theta) = A_1 r^{\lambda+1}\{\gamma_1 \cos(\lambda+1)\theta + \eta_{13} \sin(\lambda+1)\theta - \gamma_1 \cos(\lambda-1)\theta + \gamma_1\eta_1 \sin(\lambda-1)\theta\}$
		$\eta_{13} = -\frac{\gamma_1}{\sin(\lambda+1)\alpha}(\cos(\lambda+1)\alpha - \cos(\lambda-1)\alpha + \eta_1 \sin(\lambda-1)\alpha)$
9	Simply supported (I)–simply supported (II)	$\Psi_r(r,\theta) = A_2 r^{\lambda}\{\sin(\lambda+1)\theta + \frac{1}{\eta_3}\sin(\lambda-1)\theta\}$
		$\Psi_\theta(r,\theta) = A_2 r^{\lambda}\{\cos(\lambda+1)\theta + (k_2/\eta_3)\cos(\lambda-1)\theta\}$
		$W(r,\theta) = A_2 r^{\lambda+1}\{\frac{\upsilon-1}{1+\lambda+\upsilon+\lambda\upsilon}\sin(\lambda+1)\theta + (\gamma_1/\eta_3)\sin(\lambda-1)\theta\}$

Table 2 (*continued*)

Case no.	Boundary conditions	Corner functions
10	Simply supported (II)–free	$\Psi_r(r,\theta) = A_1 r^{\lambda}\{\cos(\lambda+1)\theta + \eta_{14}\sin(\lambda+1)\theta + \eta_{15}\cos(\lambda-1)\theta + \eta_{16}\sin(\lambda-1)\theta\}$ $\Psi_\theta(r,\theta) = A_1 r^{\lambda}\{-\sin(\lambda+1)\theta + \eta_{14}\cos(\lambda+1)\theta - k_2\eta_{15}\sin(\lambda-1)\theta + k_2\eta_{16}\cos(\lambda-1)\theta\}$ $W(r,\theta) = A_1 r^{\lambda+1}\{-\gamma_1\eta_{15}\cos(\lambda+1)\theta + \eta_{17}\sin(\lambda+1)\theta + \gamma_1\eta_{15}\cos(\lambda-1)\theta + \gamma_1\eta_{16}\sin(\lambda-1)\theta\}$ $\eta_{14} = -\frac{(1+k_2)(\lambda-1)}{2\lambda}\eta_{16}, \quad \eta_{15} = -\frac{-3+\lambda+\upsilon+\lambda\upsilon}{(1+\lambda)(1+\upsilon)}$ $\eta_{16} = -\frac{\lambda(1-\upsilon)\cos(\lambda+1)\alpha+\eta_{15}(k_2(\lambda-1)-\lambda\upsilon-1)\cos(\lambda-1)\alpha}{(-(1+k_2)(\lambda-1)/2)(1-\upsilon)\sin(\lambda+1)\alpha+(k_2(\lambda-1)-\lambda\upsilon-1)\sin(\lambda-1)\alpha}$ $\eta_{17} = \frac{-(1+(1+\lambda)\gamma_1\eta_{15})\sin(1+\lambda)\alpha+\eta_{15}(\lambda\gamma_1-k_2-\gamma_1)\sin(\lambda-1)\alpha}{(1+\lambda)\cos(1+\lambda)\alpha} + \frac{-(1+k_2)(\lambda-1)/(2\lambda)\cos(1+\lambda)\alpha-(\lambda\gamma_1-k_2-\gamma_1)\cos(\lambda-1)\alpha}{(1+\lambda)\cos(1+\lambda)\alpha}\eta_{16}$

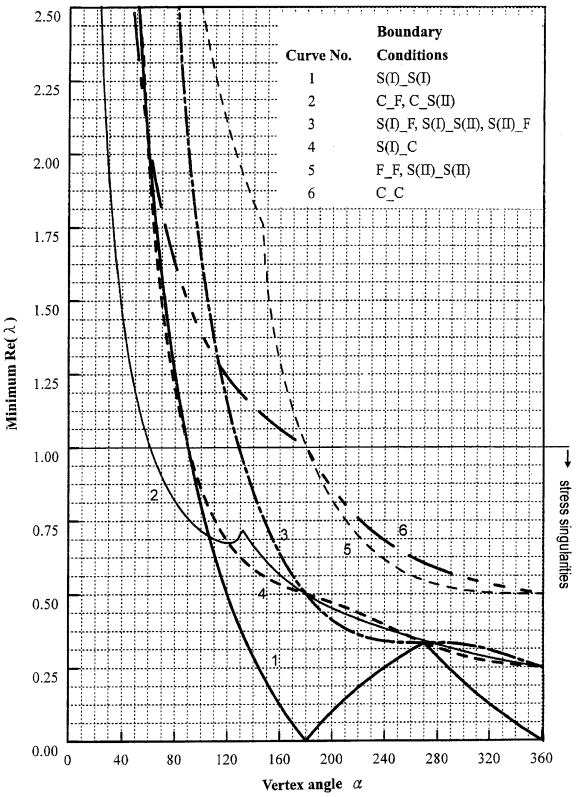

Fig. 1. Variation of minimum positive Re(λ) with vertex angle α for FSDPT.

in curves 1 and 6 arise from curve crossing. For example, when the vertex angle is below 180°, the minimum value of Re(λ) for curve 6 is determined by the characteristic equation for symmetric deformation. It is determined by the anti-symmetric case for $\alpha > 180°$. The nonsmooth parts of curves 2 and 5 where the vertex angle is around 130° for curve 2 and 145° for curve 5 are not due to curve crossing, but to the roots' changing from real to complex numbers.

Fig. 1 indicates that, regardless of the boundary conditions around the corner, no moment singularities are present if α is less than 60°, while such singularities always occur if $\alpha > \pi$. A corner with C_F and C_S(II) boundary conditions exhibits the strongest moment singularities for α less than approximately 105°, while the S(I)_S(I) boundary condition leads to the strongest moment singularities for other vertex angles. A corner with S(I)_S(I) and S(I)_C boundary conditions exhibits moment singularities for $\alpha > \pi/2$, while S(I)_F, S(I)_S(II), and S(II)_F boundary conditions result in moment singularities for α above around 128°. For boundary conditions F_F, S(II)_S(II), and C_C, moment singularities surface at $\alpha > \pi$. The strength of the singularity at the vertex increases with increasing the vertex angle, except under S(I)_S(I), C_F, and C_S(II) boundary conditions. The results for $\alpha = 2\pi$ (a sharp crack) under F_F, S(II)_S(II), and C_C boundary conditions yield an order of the moment singularity at the crack tip of $r^{-1/2}$. When $\alpha = 2\pi$, the S(I)_S(I) boundary condition yields an order of r^{-1} for, and other boundary conditions, an order of $r^{-3/4}$.

4. Singularity of shear forces

Notably, the coupled ordinary differential equations (Eqs. (5)) can also be solved by assuming the following expansions into infinite series:

$$\psi_r = \sum_{n=0} \bar{a}_{2n} r^{\bar{\lambda}+2n+1}, \quad \psi_\theta = \sum_{n=0} \bar{b}_{2n} r^{\bar{\lambda}+2n+1} \quad \text{and} \quad w = \sum_{2n=0} \bar{c}_{2n} r^{\bar{\lambda}+2n}, \tag{20}$$

where $\bar{\lambda}$ can be a complex number with a positive real part to satisfy the regularity conditions for displacement components as r approaches zero. In Eq. (20), the starting order of r in w is one less than that for r in both ψ_r and ψ_θ, such that the singularity of shear forces occurs in the vicinity of r equal to zero when Re($\bar{\lambda}$) is below unity. No moment singularity occurs. The procedure described in the previous section requires that the coefficients in Eq. (20) satisfy

$$\frac{D}{2}\{[-2+2(2m+3+\bar{\lambda})^2 + p^2(1-\upsilon)]\bar{a}_{2m+2} - p[(\bar{\lambda}+2m+3)(1+\upsilon) - 3 + \upsilon]\bar{b}_{2m+2}\}$$
$$+ \kappa^2 Gh(\bar{\lambda}+2m+2)\bar{c}_{2m+2} = \kappa^2 Gh\bar{a}_{2m}, \tag{21a}$$

$$\frac{D}{2}\{[3-\upsilon+(1+\upsilon)(\bar{\lambda}+2m+3)]p\bar{a}_{2m+2} + [(1-\upsilon)((\bar{\lambda}+2m+3)^2 + p^2 - 1)$$
$$+ (1+\upsilon)p^2]\bar{b}_{2m+2}\} + \kappa^2 Gh(p\bar{c}_{2m+2}) = \kappa^2 Gh\bar{b}_{2m}, \tag{21b}$$

$$[(\bar{\lambda}+2m+2)^2 + p^2]\bar{c}_{2m+2} = (\bar{\lambda}+2m+2)\bar{a}_{2m} + p\bar{b}_{2m} \tag{21c}$$

and

$$\frac{D}{2}\{[-2+2(1+\bar{\lambda})^2 + p^2(1-\upsilon)]\bar{a}_0 + p[(1+\bar{\lambda})(1+\upsilon) - 3 + \upsilon]\bar{b}_0\} + \kappa^2 Gh\bar{\lambda}\bar{c}_0 = 0, \tag{22a}$$

$$\frac{D}{2}\{[3-\upsilon+(1+\upsilon)(\bar{\lambda}+1)]p\bar{a}_0+[(1-\upsilon)(p^2-1+(1+\bar{\lambda})^2)+(1+\upsilon)p^2]\bar{b}_0+\kappa^2 Gh\,p\bar{c}_0=0, \quad (22b)$$

$$(\bar{\lambda}^2+p^2)\bar{c}_0=0. \quad (22c)$$

To establish a nontrivial solution for the coefficients $\bar{a}_0, \bar{b}_0$, and $\bar{c}_0$ in Eqs. (22), p must be related to $\bar{\lambda}$ by, $p=\pm\bar{\lambda}$i or $p=\pm(2+\bar{\lambda})$i. When $p=\pm\bar{\lambda}i$,

$$\bar{c}_0=-\frac{D}{2\kappa^2 Gh}\{[3-\upsilon+(1+\upsilon)(1+\bar{\lambda})]\bar{a}_0 \mp \mathrm{i}[2(1-\upsilon)-(1+\upsilon)\bar{\lambda}]\bar{b}_0\}, \quad (23)$$

and $\bar{a}_0$ and $\bar{b}_0$ are undetermined. When $p=\pm(2+\bar{\lambda})$i, $\bar{c}_0=0$ and $\bar{b}_0=\pm\mathrm{i}\bar{a}_0$.

Consequently, the general asymptotic form for the displacement components near the vertex can be expressed as

$$\Psi_r(r,\theta)=[\bar{A}_1\cos\bar{\lambda}\theta+\bar{A}_2\sin\bar{\lambda}\theta+\bar{A}_3\cos(2+\bar{\lambda})\theta+\bar{A}_4\sin(2+\bar{\lambda})\theta]r^{\bar{\lambda}+1}+O(r^{\bar{\lambda}+3}), \quad (24a)$$

$$\Psi_\theta(r,\theta)=[\bar{B}_1\cos\bar{\lambda}\theta+\bar{B}_2\sin\bar{\lambda}\theta+\bar{A}_4\cos(2+\bar{\lambda})\theta-\bar{A}_3\sin(2+\bar{\lambda})\theta]r^{\bar{\lambda}+1}+O(r^{\bar{\lambda}+3}), \quad (24b)$$

$$W(r,\theta)=[\bar{l}_1(\bar{A}_1\cos\bar{\lambda}\theta+\bar{A}_2\sin\bar{\lambda}\theta)+\bar{l}_2(\bar{B}_2\cos\bar{\lambda}\theta-\bar{B}_1\sin\bar{\lambda}\theta)]r^{\bar{\lambda}}+O(r^{\bar{\lambda}+2}), \quad (24c)$$

where

$$\bar{l}_1=\frac{-D}{2\kappa^2 Gh}(3-\upsilon+(1+\upsilon)(1+\bar{\lambda})) \quad \text{and} \quad \bar{l}_2=\frac{D}{2\kappa^2 Gh}(2(1-\upsilon)-(1+\upsilon)\bar{\lambda}).$$

The coefficients $\bar{A}_1, \bar{A}_2, \bar{A}_3, \bar{A}_4, \bar{B}_1$, and $\bar{B}_2$ are determined from the boundary conditions.

Let us consider a sector plate with type I simply supported (Eq. (15c)) radial edges, to demonstrate finding the characteristic equation for $\bar{\lambda}$, and determining the corresponding corner functions. By symmetry, substituting Eqs. (24) into Eq. (15c) yields the following equations for symmetric deformation:

$$\bar{l}_1\bar{A}_1\cos\bar{\lambda}\alpha/2+\bar{l}_2\bar{B}_2\cos\bar{\lambda}\alpha/2=0, \quad (25a)$$

$$\bar{A}_1\cos\bar{\lambda}\alpha/2+\bar{A}_3\cos\bar{\lambda}\alpha/2=0, \quad (25b)$$

$$(1+\upsilon+\upsilon\bar{\lambda})\bar{A}_1\cos\bar{\lambda}\alpha/2+(1+\bar{\lambda})(\upsilon-1)\bar{A}_3\cos(\bar{\lambda}+2)\alpha/2+\bar{B}_2\bar{\lambda}\cos\bar{\lambda}\alpha/2=0. \quad (25c)$$

The following characteristic equation ensures a nontrivial solution for $\bar{A}_1$, $\bar{A}_3$, and $\bar{B}_2$:

$$(\cos\bar{\lambda}\alpha/2)^2\cos(\bar{\lambda}+2)\alpha/2=0. \quad (26)$$

When $\cos\bar{\lambda}\alpha/2=0$, Eqs. (25) result in $\bar{A}_3=0$, and leave $\bar{A}_1$ and $\bar{B}_2$ undetermined. The corresponding corner functions are

$$\Psi_r(r,\theta)=\bar{A}_1\gamma^{\bar{\lambda}+1}\cos\bar{\lambda}\theta, \quad \Psi_\theta(r,\theta)=\bar{B}_2 r^{\bar{\lambda}+1}\sin\bar{\lambda}\theta, \quad W(r,\theta)=r^{\bar{\lambda}}(\bar{l}_1\bar{A}_1+\bar{l}_2\bar{B}_2)\cos\bar{\lambda}\theta. \quad (27)$$

When $\cos(\bar{\lambda}+2)\alpha/2=0$, Eqs. (25) result in $\bar{A}_1=\bar{B}_2=0$ and leave $\bar{A}_3$ undetermined, so that the coefficient of $r^{\bar{\lambda}}$ in Eq. (24c) equals zero. The solution obtained from Eqs. (20) degenerates to the form of Eq. (6), yielding no singularities of shear forces. Consequently, $\cos(\bar{\lambda}+2)\alpha/2=0$ is not a characteristic equation for the shear-force singularity.

Similarly, $\bar{\lambda}$ must satisfy the following equation to ensure a nontrivial solution for anti-symmetric deformation:

$$(\sin\bar{\lambda}\alpha/2)^2\sin(\bar{\lambda}+2)\alpha/2=0. \tag{28}$$

Again, $\sin(\bar{\lambda}+2)\alpha/2=0$ yields $\bar{A}_2=\bar{B}_1=0$, such that the solution given by Eq. (20) degenerates into the form of Eq. (6). When $\sin\bar{\lambda}\alpha/2=0$, the corresponding corner functions are

$$\Psi_r(r,\theta)=\bar{A}_2\gamma^{\bar{\lambda}+1}\sin\bar{\lambda}\theta,\quad \Psi_\theta(r,\theta)=\bar{B}_1 r^{\bar{\lambda}+1}\cos\bar{\lambda}\theta,\quad W(r,\theta)=r^{\bar{\lambda}}(\bar{l}_1\bar{A}_2-\bar{l}_2\bar{B}_1)\sin\bar{\lambda}\theta. \tag{29}$$

The characteristic equations of $\bar{\lambda}$ and the corresponding corner functions for various boundary conditions can be derived by following the procedure given above. Table 3 collates the characteristic equations for $\bar{\lambda}$, resulting in singularities of shear forces, and the corresponding corner functions for various boundary conditions. Notably, for example, neither the corner functions given by Eq. (29) nor the corresponding characteristic equation of $\bar{\lambda}$ are listed in Table 3, because the positive roots of that characteristic equation, $\sin\bar{\lambda}\alpha/2=0$, exceed one and do not lead to a singularity of shear forces.

Notably, the characteristic equations for $\bar{\lambda}$ corresponding to the boundary conditions C_C and S(I)_C result in the leading order of Ψ_θ in Eq. (24b) vanish.

The positive roots of the characteristic equations in Table 3 are easily determined. The positive roots of $\cos\bar{\lambda}\alpha/2=0$ are $\bar{\lambda}=(2n+1)\pi/\alpha$ and $n=0,1,2,\ldots$, such that a shear-force singularity is produced when $\alpha>\pi$. The positive roots of $\cos\bar{\lambda}\alpha=0$ and $\sin\bar{\lambda}\alpha=0$ are $\bar{\lambda}=(2n+1)\pi/2\alpha$ and $\bar{\lambda}=(n+1)\pi/\alpha$, respectively, with $n=0,1,2,\ldots$. Consequently, these roots result in a shear-force singularity when $\alpha>\pi/2$ and when $\alpha>\pi$, respectively. Fig. 2 presents the smallest positive roots for each characteristic equation as α is varied.

Positive roots of characteristic equations, smaller than unity, lead to singularities of shear forces with the singular order of $\bar{\lambda}-1$. Fig. 2 reveals that if the boundary conditions around the vertex produce shear-force singularities, those singularities are stronger for a larger α. Of all the various boundary conditions, C_F, S(I)_F, and S(II)_F cause the strongest singularities for shear forces at the vertex.

5. Comparisons

The singularity behaviors of moments and shear forces from type I simply supported boundary conditions are compared with those obtained by Huang et al. [15], to verify the derivation in this study. Those authors developed an exact solution in terms of Bessel functions for the free vibrations of Mindlin sectorial plates with simply supported radial edges. Their results indicated that when $\pi/2<\alpha<\pi$, the singularity order of moments is $\pi/\alpha-2$, and no shear-force singularity is present. When $\pi<\alpha\leqslant 3\pi/2$ and $3\pi/2\leqslant\alpha<2\pi$, the singularity orders of moments are $-\pi/\alpha$ and $2\pi/\alpha-2$, respectively. When $\pi<\alpha<2\pi$, the singularity order of shear forces is $\pi/\alpha-1$.

According to curve 6 in Fig. 1, which presents the smallest positive $\mathrm{Re}(\lambda)$ for S(I)_S(I); the minimum $\mathrm{Re}(\lambda)$ for $\alpha\leqslant\pi$ is obtained from the roots of $\cos(\lambda+1)\alpha/2=0$ and is equal to $\lambda=\pi/\alpha-1$, while for $\pi<\alpha\leqslant 3\pi/2$, the minimum $\mathrm{Re}(\lambda)$ is obtained from the roots of $\cos(\lambda-1)\alpha/2=0$ and is equal to $\lambda=-\pi/\alpha+1$. Furthermore, for $3\pi/2\leqslant\alpha<2\pi$, the minimum $\mathrm{Re}(\lambda)$ is determined from

Table 3
Characteristic equations and the corresponding corner functions for the singularities of shear forces

Case no.	Boundary conditions	Characteristic equations	Corner functions
1	S(I)–S(I)	$\cos\bar{\lambda}\alpha/2=0$ (S^*)	$\Psi_r(r,\theta)=\bar{A}_1\gamma^{\bar{\lambda}+1}\cos\bar{\lambda}\theta,\ \Psi_\theta(r,\theta)=\bar{B}_2 r^{\bar{\lambda}+1}\sin\bar{\lambda}\theta$ $W(r,\theta)=r^{\bar{\lambda}}(\bar{l}_1\bar{A}_1+\bar{l}_2\bar{B}_2)\cos\bar{\lambda}\,\theta$
2	C–F	$\cos\bar{\lambda}\alpha=0$	$\Psi_r(r,\theta)=\bar{A}_1 r^{\bar{\lambda}+1}\{\cos\bar{\lambda}\theta+\bar{\eta}_1\sin\bar{\lambda}\theta-\cos(2+\bar{\lambda})\theta+\bar{\eta}_2\sin(2+\bar{\lambda})\theta\}$ $\Psi_\theta(r,\theta)=\bar{A}_1 r^{\bar{\lambda}+1}\{-\bar{\eta}_2\cos\bar{\lambda}\theta-\frac{\bar{l}_1}{\bar{l}_2}\sin\bar{\lambda}\theta+\bar{\eta}_2\cos(2+\bar{\lambda})\theta+\sin(2+\bar{\lambda})\theta\}$ $W(r,\theta)=\bar{A}_1(\bar{l}_1\bar{\eta}_1+\bar{l}_2\bar{\eta}_2)r^{\bar{\lambda}}\sin\bar{\lambda}\theta$ $\bar{\eta}_1=-\frac{-(1+\bar{\lambda})(\upsilon-1)\cos(\bar{\lambda}+2)\alpha+\bar{\eta}_2((1+\bar{\lambda})(\upsilon-1)\sin(\bar{\lambda}+2)\alpha+\bar{\lambda}\sin\bar{\lambda}\ \alpha)}{(1+\upsilon+\bar{\lambda}\upsilon)\sin\bar{\lambda}\alpha}$ $\bar{\eta}_2=\frac{(1+\bar{l}_1/\bar{l}_2)\bar{\lambda}\sin\bar{\lambda}\alpha-2(1+\bar{\lambda})\sin(\bar{\lambda}+2)\alpha}{2(1+\bar{\lambda})\cos(\bar{\lambda}\ +2)\alpha}$
3	S(I)–F	$\cos\bar{\lambda}\alpha=0$	$\Psi_r(r,\theta)=\bar{A}_2 r^{\bar{\lambda}+1}\sin\bar{\lambda}\theta,\quad \Psi_\theta(r,\theta)=\frac{(1+\upsilon+\bar{\lambda}\upsilon)}{\bar{\lambda}}\bar{A}_2 r^{\bar{\lambda}+1}\cos\bar{\lambda}\ \theta$ $W(r,\theta)=\bar{A}_2\left(\bar{l}_1-\frac{\bar{l}_2(1+\upsilon+\bar{\lambda}\upsilon)}{\bar{\lambda}}\right)r^{\bar{\lambda}}\ \sin\bar{\lambda}\theta$
4	S(I)–C	$\sin\bar{\lambda}\alpha=0$	$\Psi_r(r,\theta)=\bar{A}_2 r^{\bar{\lambda}+1}\sin\bar{\lambda}\theta,\quad W(r,\theta)=\bar{A}_2\bar{l}_1 r^{\bar{\lambda}}\sin\bar{\lambda}\theta$
5	F–F	$\cos\bar{\lambda}\alpha/2=0$ (A^*)	$\Psi_r(r,\theta)=\bar{A}_2 r^{\bar{\lambda}+1}\sin\bar{\lambda}\theta,\quad \Psi_\theta(r,\theta)=\frac{(1+\upsilon+\bar{\lambda}\upsilon)}{\bar{\lambda}}\bar{A}_2 r^{\bar{\lambda}\ +1}\cos\bar{\lambda}\theta$ $W(r,\theta)=\bar{A}_2\left(\bar{l}_1-\frac{\bar{l}_2(1+\upsilon+\bar{\lambda}\upsilon)}{\bar{\lambda}}\right)r^{\bar{\lambda}}\ \sin\bar{\lambda}\theta$
6	C–C	$\cos\bar{\lambda}\alpha/2=0$ (S^*)	$\Psi_r(r,\theta)=\bar{A}_1\gamma^{\bar{\lambda}+1}\cos\bar{\lambda}\theta,\quad W(r,\theta)=\bar{A}_1\bar{l}_1 r^{\bar{\lambda}}\cos\bar{\lambda}\theta$
7	S(II)–S(II)	$\cos\bar{\lambda}\alpha/2=0$ (S^*)	$\Psi_r(r,\theta)=\bar{A}_1\gamma^{\bar{\lambda}+1}\cos\bar{\lambda}\theta,\quad \Psi_\theta(r,\theta)=\bar{A}_1 r^{\bar{\lambda}+1}\sin\bar{\lambda}\theta$ $W(r,\theta)=\bar{A}_1(\bar{l}_1+\bar{l}_2)r^{\bar{\lambda}}\cos\bar{\lambda}\theta$
8	C–S(II)	$\sin\bar{\lambda}\alpha=0$	$\Psi_r(r,\theta)=\bar{A}_1 r^{\bar{\lambda}+1}\{\cos\bar{\lambda}\theta+\bar{\eta}_3\sin\bar{\lambda}\theta-\cos(2+\bar{\lambda})\theta+\bar{\eta}_4\sin(2+\bar{\lambda})\theta\}$ $\Psi_\theta(r,\theta)=\bar{A}_1 r^{\bar{\lambda}+1}\left\{-\bar{\eta}_4\cos\bar{\lambda}\theta-\frac{\bar{l}_1}{\bar{l}_2}\sin\bar{\lambda}\theta+\bar{\eta}_4\cos(2+\bar{\lambda})\theta+\sin(2+\bar{\lambda})\theta\right\}$ $W(r,\theta)=\bar{A}_1(\bar{l}_1\bar{\eta}_3+\bar{l}_2\bar{\eta}_4)r^{\bar{\lambda}}\sin\bar{\lambda}\theta$ $\bar{\eta}_3=-\frac{2(1+\bar{\lambda})\sin(\bar{\lambda}+2)\alpha+\bar{\eta}_4(2(1+\bar{\lambda})\cos(\bar{\lambda}+2)\alpha-\bar{\lambda}\cos\bar{\lambda}\alpha)}{\bar{\lambda}\cos\bar{\lambda}\ \alpha}$ $\bar{\eta}_4=-\frac{(1+\upsilon+\upsilon\bar{\lambda})\cos\bar{\lambda}\alpha-(1+\bar{\lambda})(\upsilon-1)\cos(2+\bar{\lambda})\alpha-(\bar{l}_1/\bar{l}_2)\bar{\lambda}\cos\bar{\lambda}\alpha}{(1+\bar{\lambda})(\upsilon-1)\sin(2+\bar{\lambda}\ )\alpha}$
9	S(I)–S(II)	$\sin\bar{\lambda}\alpha=0$	$\Psi_r(r,\theta)=\bar{A}_2 r^{\bar{\lambda}+1}\sin\bar{\lambda}\theta$ $\Psi_\theta(r,\theta)=-\bar{A}_2 r^{\bar{\lambda}+1}\cos\bar{\lambda}\theta$ $W(r,\theta)=\bar{A}_2(\bar{l}_1+\bar{l}_2)r^{\bar{\lambda}}\sin\bar{\lambda}\theta$
10	S(II)–F	$\cos\bar{\lambda}\alpha=0$	$\Psi_r(r,\theta)=\bar{A}_1 r^{\bar{\lambda}+1}\{\cos\bar{\lambda}\theta+\bar{\eta}_5\sin\bar{\lambda}\theta+\bar{\eta}_6\cos(2+\bar{\lambda})\theta+\bar{\eta}_7\sin(2+\bar{\lambda})\theta\}$ $\Psi_\theta(r,\theta)=\bar{A}_1 r^{\bar{\lambda}+1}\left\{\bar{\eta}_8\cos\bar{\lambda}\theta-\frac{\bar{l}_1}{\bar{l}_2}\sin\bar{\lambda}\theta+\bar{\eta}_7\cos(2+\bar{\lambda})\theta-\bar{\eta}_6\sin(2+\bar{\lambda})\theta\right\}$

Table 3 (*continued*)

Case no.	Boundary conditions	Characteristic equations	Corner functions
			$W(r,\theta)=\bar{A}_1(\bar{I}_1\bar{\eta}_5-\bar{I}_2\bar{\eta}_8)r^{\bar{\lambda}}\sin\bar{\lambda}\theta$
			$\bar{\eta}_5=-\frac{\bar{\eta}_6(1+\bar{\lambda})(\upsilon-1)\cos(\bar{\lambda}+2)\alpha+\bar{\eta}_7(1+\bar{\lambda})(\upsilon-1)\sin(\bar{\lambda}+2)\alpha+2(1+\bar{\lambda})\bar{\eta}_7\sin\bar{\lambda}\alpha}{(1+\upsilon+\bar{\lambda}+\upsilon\bar{\lambda})\sin\bar{\lambda}\ \alpha}$
			$\bar{\eta}_6=-\frac{1+\upsilon+\bar{\lambda}\upsilon-(\bar{I}_1/\bar{I}_2)\bar{\lambda}}{(1+\bar{\lambda}\ )(\upsilon-1)}$
			$\bar{\eta}_7=\frac{(1+\bar{I}_1/\bar{I}_2)\bar{\lambda}\sin\bar{\lambda}\alpha+2\bar{\eta}_6(1+\bar{\lambda})\sin(2+\bar{\lambda})\alpha}{2(1+\bar{\lambda})\cos(2+\bar{\lambda}\ )\alpha}$
			$\bar{\eta}_8=-\left(\bar{\eta}_5+\frac{2(1+\bar{\lambda})\bar{\eta}_7}{\bar{\lambda}}\right)$

Note: $^*S$—symmetric case, A—anti-symmetric case.

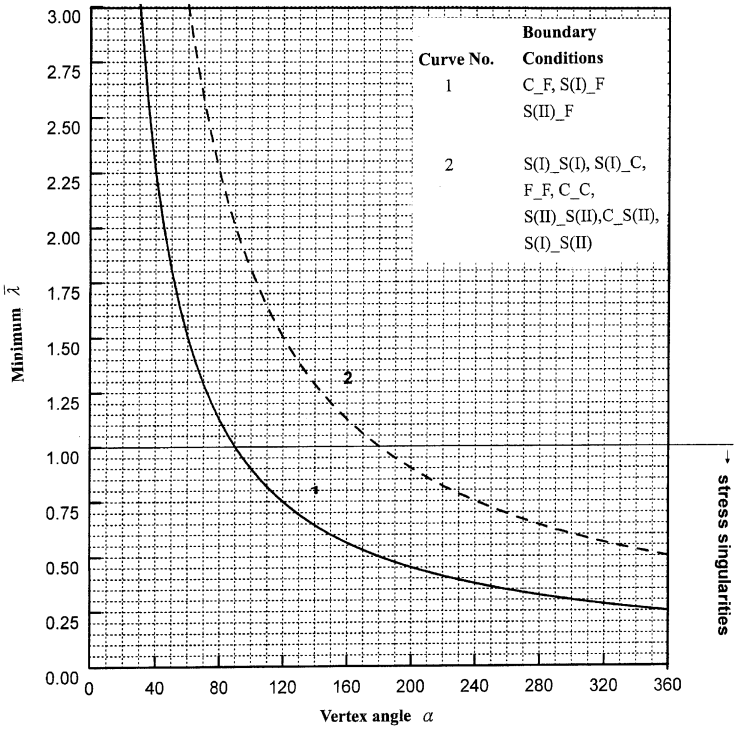

Fig. 2. Variation of minimum positive $\bar{\lambda}$ with vertex angle α for FSDPT.

the roots of $\sin(\lambda+1)\alpha/2=0$ and is equal to $\lambda=2\pi/\alpha-1$. Consequently, our results display the exactly same singularity behaviors of moments as did those of Huang et al. [15].

Fig. 2 indicates that, for the shear-force singularities, the smallest positive $\bar{\lambda}$ under S(I)_S(I) boundary conditions is equal to π/α, corresponding exactly to the same shear-force singularities as found by Huang et al. [15].

The characteristic equations from FSDPT can be interestingly compared with those from three-dimensional elasticity theory. Hartranft and Sih [20] obtained the following characteristic equations for a complete free wedge, according to a three-dimensional elasticity approach:

$$\sin\lambda\alpha = \lambda\sin\alpha, \tag{30a}$$

$$\sin\lambda\alpha = \lambda\sin\alpha, \tag{30b}$$

$$\lambda = 2n\pi/\alpha \tag{30c}$$

$$\text{or } \lambda = (2n+1)\pi/\alpha, \tag{30d}$$

where $n = 0, 1, 2, 3\ldots$. Notably, Eq. (30c) results in no stress singularities because λ exceeds unity. The characteristic equations (30a) and (30b), and the values of λ specified by Eq. (30d) are exactly the same as those obtained in the present study for F_F boundary conditions (see Tables 1 and 3).

Table 1 also presents the characteristic equations of CPT for various boundary conditions given by Williams [4], to compare the singularity behaviors from the FSDPT with those from CPT. At first sight, one might conclude that with the same boundary conditions the characteristic equations for FSDPT are completely different from those for CPT. However, carefully investigating the case for S(I)_S(I) boundary conditions, reveals that both theories give the same characteristic equations for this case. Using trigonometric identities, $(\cos(\lambda-1)\alpha/2)(\cos(\lambda+1)\alpha/2) = 0$ can be reduced to $\cos\alpha\lambda = -\cos\alpha$, and $(\sin(\lambda-1)\alpha/2)(\sin(\lambda+1)\alpha/2) = 0$ can be reduced to $\cos\alpha\lambda = +\cos\alpha$. Interestingly, some of the characteristic equations for CPT have appeared in FSDPT, but with different boundary conditions. For example, the characteristic equation for S(I)_C boundary conditions in CPT is equivalent to that for S(I)_F boundary conditions in FSDPT. Fig. 3 plots the minimum positive values of $\mathrm{Re}(\lambda)$ for different α from the characteristic equations for CPT, not shown in FSDPT, to compare the singularity orders under the same boundary conditions.

Fig. 3 shows that for C_F boundary conditions, FSDPT exhibits stronger moment singularity than the classical plate theory exhibits for α less than approximately 130°, while for α larger than 130°, the opposite is observed. For S(I)_F boundary conditions, FSDPT presents stronger moment singularity than does CPT for $180° < \alpha < 270°$, while the opposite holds for other value of α. Fig. 3 also shows that FSDPT has stronger moment singularity than has CPT under F_F boundary conditions. Furthermore, comparing curves 4 and 3 of Fig. 1 reveals that for S(I)_C boundary conditions, CPT has stronger moment singularity than has FSDPT for $180° < \alpha < 270°$, while the opposite holds for other values of α. Comparing curves 6 and 5 in Fig. 1 shows that for C_C boundary conditions, CPT has stronger moment singularity than has FSDPT.

CPT does not account for shear deformation so the shear forces are determined from the equilibrium equations. The shear-force singularity is always stronger than the moment singularity. The singularity order of shear forces is one below that for moments. Subsequently, the shear-force singularity for CPT is stronger than that for FSDPT.

The characteristic equations for cases 1–6 in Table 1 are exactly the same as the results obtained by Burton and Sinclair [14] for Reissner's theory, but with somewhat different expressions. However, these authors did not consider the boundary conditions in cases 7–10 in Table 1 in this paper. Moreover, no shear-force singularity is contained in their solution, exposing their solution's incompleteness.

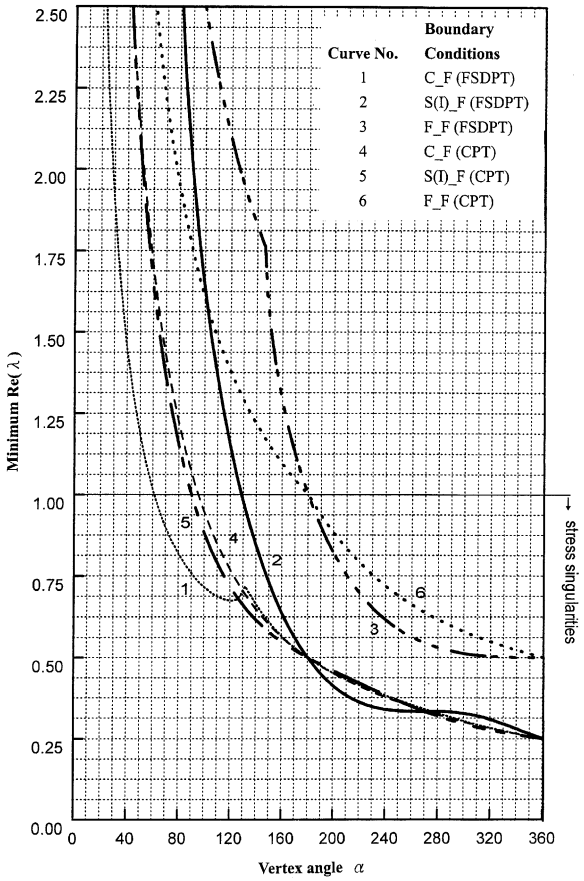

Fig. 3. Comparison of minimum positive Re(λ) for FSDPT and CPT.

Finally, the characteristic equations for C_C, C_F, and F_F given in Table 1 obtained in this work, are exactly the same as those for plates under extension with the same boundary conditions, as were obtained by Williams [5].

6. Concluding remarks

This investigation has presented the Williams-type asymptotic solution at a corner of a thick plate with various boundary conditions using an eigenfunction expansion technique to solve the three partial differential equations for displacement components in FSDPT. The characteristic equations for determining the singularity orders for moments and shear forces at the corner, with corresponding corner functions for various boundary conditions, were also fully developed. Notably, under identical boundary conditions, the equations characterizing the singularity behaviors of moments are totally different from those characterizing the singularity behaviors of shear forces.

The validity of the solution was confirmed by comparing the moment and shear-force singularity behaviors for type I simply supported conditions with those from the exact solution of free vibrations of a sector plate with the same boundary conditions along radial edges. Furthermore, the obtained characteristic equations for a free–free boundary condition were consistent with those for a completely free wedge from three-dimensional elasticity solution.

The characteristic equations for FSDPT are completely different from those for the classical thin plate theory, except in the case of simply supported (S(I)) radial edges. The boundary conditions and the vertex angle determine which theory, FSDPT or CPT, produces a stronger moment singularity. Nevertheless, the classical theory always leads to a stronger shear-force singularity than does the FSDPT because the former does not consider the shear deformation.

The obtained characteristic equations demonstrate that the free boundary condition and the type II simply supported boundary condition affect the moment singularity in the same way. The presented results also show that the radial boundary conditions generate no moment singularity when the vertex angle is below approximately 60°, while moment singularity always occurs when the vertex angle exceeds 180°. C_F boundary conditions produce the strongest moment singularity among the various boundary conditions when the vertex angle is less than approximately 105°, while S(I)-S(I) boundary conditions lead to the strongest singularity for other angles. The fixed radial edges generate the weakest moment singularity.

The shear-force singularity generated by various boundary conditions occurs only when the vertex angle exceeds 90°. The radial C_F, S(I)_F, or S(II)_F boundary conditions result in the same shear-force singularity as occurs when the vertex angle is larger than 90°.

The corner functions corresponding to various boundary conditions presented here can be applied to numerical analysis for the complex problems of moderately thick plates with corner singularities. McGee et al. [22] and Leissa et al. [3] applied the Ritz method using the corner functions for classical plate theory as admissible functions to examine the free vibrations of skewed plates and sectorial plates.

Acknowledgements

This work reported herein was supported by the National Science Council, ROC through research grant no. NSC91-2211-E-009-039. This support is gratefully acknowledged.

References

[1] Williams ML. Stress singularity, adhesion, and fracture. Proceeding of Fifth US National Congress of Applied Mechanics, Minneapolis, Minnesota, 1966. p. 451–64.
[2] Bartholomew P. Solution of elastic crack problems by superposition of finite element and singular field. Computer Methods in Applied Mechanics and Engineering 1978;13(4):59–78.
[3] Leissa AW, McGee OG, Huang CS. Vibrations of sectorial plates having corner stress singularities. Journal of Applied Mechanics 1993;60(1):134–40.
[4] Williams ML. Stress singularities resulting from various boundary conditions in angular corners of plates under bending. Proceeding of First US National Congress of Applied Mechanics, 1952. p. 325–9.
[5] Williams ML. Stress singularities resulting from various boundary conditions in angular corners of plates in extension. Journal of Applied Mechanics 1952;19(4):526–8.

[6] Williams ML, Chapkis RL. Stress singularities for a sharp-notched polarly orthotropic plate. Proceeding of Third US National Congress of Applied Mechanics, Providence, Rhode Island 1958. p. 281–6.
[7] Dempsey JP, Sinclair GB. On the stress singularities in the plate elasticity of the composite wedge. Journal of Elasticity 1979;9(4):373–91.
[8] Hein VL, Erdogan F. Stress singularities in a two-material wedge. International Journal of Fracture Mechanics 1971;7(3):317–30.
[9] Bogy DB, Wang KC. Stress singularities at interface corners in bonded dissimilar isotropic elastic materials. International Journal of Solids and Structure 1971;7(10):993–1005.
[10] Dempsey JP, Sinclair GB. On the stress singular behavior at the vertex of a bi-material wedge. Journal of Elasticity 1981;11(3):317–27.
[11] Ting TCT, Chou SC. Edge singularities in anisotropic composites. International Journal of Solids and Structures 1981;17(11):1057–68.
[12] Stroh AN. Steady state problems in anisotropic elasticity. Journal of Mathematics and Physics 1962;41(2):77–103.
[13] Ojikutu IO, Low RO, Scott RA. Stress singularities in laminated composite wedge. International Journal of Solids and Structures 1984;20(8):777–90.
[14] Burton WS, Sinclair GB. On the singularities in Reissner's theory for the bending of elastic plates. Journal of Applied Mechanics 1986;53:220–2.
[15] Huang CS, Leissa AW, McGee OG. Exact analytical solutions for the vibrations of Mindlin sectorial plates with simply supported radial edges. International Journal of Solid and Structures 1994;31(11):1609–31.
[16] Reissner E. The effect of transverse shear deformation on the bending of elastic plates. Journal of Applied Mechanics 1945;12:69–77.
[17] Mindlin RD. Influence of rotatory inertia and shear on flexural motion of isotropic, elastic plates. Journal of Applied Mechanics 1951;18:31–8.
[18] Xie M, Chaudhuri RA. Three-dimensional stress singularity at a bimaterial interface crack front. Composite Structures 1998;40(2):137–47.
[19] Chaudhuri RA, Xie M. A novel eigenfunction expansion solution for three-dimensional crack problems. Composite Science and Technology 2000;60:2565–80.
[20] Hartranft RJ, Sih GC. The use of eigenfunction expansions in the general solution of three-dimensional crack problems. Journal of Mathematics and Mechanics 1969;19(2):123–38.
[21] Mindlin RD, Deresiewicz H. Thickness-shear and flexural vibrations of a circular disk. Journal of Applied Physics 1954;25:1329–32.
[22] McGee OG, Leissa AW, Huang CS. Vibrations of cantilevered skewed plates with corner stress singularities. International Journal of Numerical Methods in Engineering 1992;35(2):409–24.